Bounding Uncertainty in State Estimation Under Dynamic Event-Triggered Communication

Irene Perez-Salesa, *Graduate Student Member, IEEE*,
Rodrigo Aldana-López, *Graduate Student Member, IEEE*, and Carlos Sagüés, *Senior Member, IEEE*

***Abstract*—In the stochastic estimation context, the absence of measurement information at the state estimator during large intervals can cause a divergence in the uncertainty of the estimates. This issue is aggravated when strategies to reduce communication, such as event-triggering mechanisms (ETMs), are used if an appropriate design is not made. Particularly, dynamic ETMs (DETMs) may exhibit this problem, since they are designed to further reduce the number of communication instants. Motivated by this problem, we propose a novel state estimator that integrates discrete transmitted measurements and implicit information between events provided by the proposed DETM. Our proposal guarantees a uniformly bounded mean-squared error in the stochastic context, regardless of transmission instants. Moreover, compared to static ETMs, our proposal adaptively reduces the number of transmissions according to the behavior of the measured signal. Our proposal's advantages are verified formally and through several numerical experiments.**

***Index Terms*—Estimation and filtering, event-triggered communication, remote state estimation, stochastic systems.**

I. Introduction

EVENT-TRIGGERING mechanisms (ETMs) aim to reduce the computational and communication burden in systems with limited resources. In the context of remote state estimation, these strategies determine whether sensor data should be transmitted to the estimator, considering the cost of communication. In networked systems, communication bandwidth is often limited and shared, making ETMs crucial for efficient operation [1].

Reducing the amount of transmitted data is of great interest, but often requires a tradeoff between the communication rate and the quality of estimation [2]. To ensure that the quality of the estimation in the remote estimator remains within some desired bounds, most works monitor it in the triggering condition. This approach uses a local copy of the estimator at the sensor side, choosing to send data according to the mean estimation error [3], the measured value deviating from the prediction [4], [5], [6], the local estimate deviating from the remote one [7], [8], or the predicted variance of the measurement [9]. This last option ensures a bounded estimation uncertainty. However, relying only on monitoring the variance of the estimation may result in periodic transmissions, limiting the benefits of ETMs. Furthermore, implementing local estimators in sensor nodes may not be feasible due to resource limitations.

Other ETMs rely only on the sensor's measurements, such as the send-on-delta (SOD) rule, which consists of transmitting information only when the difference between the current measured value and the last transmitted one exceeds a constant threshold [1]. Thus, transmission instants are adapted according to the measured output, which may result in a reduction of communication burden compared to triggers that do not monitor the current output of the system [10].

To further reduce the number of transmissions, some works use dynamic ETMs (DETMs), which include an additional dynamic variable that enlarges the triggering threshold with respect to static triggers such as SOD. Furthermore, the introduction of the dynamic threshold and the trigger parameters grants more flexibility to adapt to a desired performance given available resources. This is, DETMs adaptively reduce transmissions in comparison to static ETMs, taking into account the characteristics of the measured signal. We refer the reader to [11] for further discussion on the advantages of DETMs and a visual example of such behavior. DETMs have been recently applied to state estimation [12], [13], [14], [15], by making the dynamic threshold depend on the sensor's measurements. However, measurement-based triggers do not guarantee an acceptable estimate in the remote estimator, particularly in the stochastic context, as they do not monitor the estimation performance. For this reason, works featuring DETMs typically assume no noise in the system [14], or consider only bounded noise [16], [17], [18]. To the best of our knowledge, the effect of DETMs has not been studied in the stochastic context.

For measurement-based triggers, if it is assumed that there is no new available data for the system between events, a model-based prediction can be used in the stochastic context. However, in the stochastic setting, the estimation uncertainty (usually given in terms of an error covariance matrix for the estimates) may grow unbounded as the time between events

Received 4 July 2024; accepted 6 September 2024. Date of publication 3 October 2024; date of current version 18 December 2024. This work was supported in part by the MCIN/AEI/10.13039/501100011033, by ERDF a way of making Europe, and by the European Union NextGenerationEU/PRTR under Project PID2021-124137OB-I00 and Project TED2021-130224B-I00; in part by the Gobierno de Aragón under Project DGA T45-23R; in part by the Universidad de Zaragoza and Banco Santander; in part by the Consejo Nacional de Ciencia y Tecnología (CONACYT-Mexico) under Grant 739841; and in part by Ministerio de Universidades under Grant FPU20/03134. This article was recommended by Associate Editor M. Basin.
(Corresponding author: Irene Perez-Salesa.)

The authors are with the Departamento de Informática e Ingeniería de Sistemas and the Instituto de Investigación en Ingeniería de Aragón, Universidad de Zaragoza, 50018 Zaragoza, Spain (e-mail: i.perez@unizar.es).
Color versions of one or more figures in this article are available at https://doi.org/10.1109/TSMC.2024.3465232.

Digital Object Identifier 10.1109/TSMC.2024.3465232

increases, because of the unknown timing of the next event. This problem is particularly relevant for unstable systems, for which a bounded input can produce an unbounded output, such as integrators, which are commonly used to model the movement of a target object in tracking applications. Nevertheless, if the estimator knows the triggering condition used by the sensor, it can infer additional information about the current measurement between events by considering the *negative information* implicit in the unmet triggering condition. To address this challenge, an event-based state estimator (EBSE) has been proposed in [19], which incorporates this negative information and maintains bounded estimation uncertainty at interevent intervals. This EBSE is based on Kalman filtering and ellipsoidal approximations of negative information, which is modeled for the SOD trigger and an ETM based on the Kullback–Leibler divergence. Other works have adopted similar ellipsoidal approaches for discrete-time set-membership estimators with multiple sensor measurements, such as the set-valued Kalman filter [20] or the set-membership information filter in [21], which consider static SOD triggers as well. Negative information has also been exploited in works featuring stochastic triggers [22], [23], but these often yield higher estimation errors compared to deterministic triggers with the same communication rate [24].

The use of negative information in remote state estimation has not yet been extended to the novel DETMs. Given the increased length of the interevent intervals produced by DETMs, the remote estimator would benefit from using negative information to improve the estimates between the sparse transmissions of information. However, to use negative information, the remote estimator must be aware of the triggering condition between events. Traditional DETM designs cannot provide this information, since the dynamic variable evolves according to the real-time measurement, which is unknown to the remote estimator between events. Thus, existing DETMs are unsuitable for obtaining negative information, which motivates a new design.

Motivated by this discussion, this work focuses on event-triggered remote estimation for continuous-time linear systems in a stochastic context. Our goal is to increase the time interval between triggered events to reduce communication load, without having an unbounded uncertainty of the estimate. Our contributions are as follows.

1) A new DETM design suitable for stochastic environments, which allows the use of negative information at the estimator, as opposed to the existing designs [11], while maintaining an adaptive reduction in communication.
2) An analysis of the DETM in the presence of stochastic noise, resulting in a boundedness analysis for the dynamic variable in this context.
3) A hybrid EBSE, that incorporates discrete measurements and continuous negative information, which improves the results from [19] due to the hybrid information update and a less conservative approximation of the negative information.
4) An analysis of boundedness of the uncertainty for all time, in terms of the error covariance of the estimates, as well as proof of consistency in the sense that the real covariance is contained within our uncertainty bound.
5) In-depth simulation examples and discussions to validate our proposal and compare them to other approaches, namely, static and variance-based ETMs [1], [9], estimation through standard Kalman filtering, and the EBSE from [19].

A. Notation

Let $\|\bullet\|$ represent the Euclidean norm for vectors and the matrix norm induced by the Euclidean norm for matrices. $\mathbb{P}(\bullet)$ represents a probability measure. The chi distribution of n degrees of freedom and noncentrality parameter λ is denoted as $\chi(n,\lambda)$. The normal distribution of mean μ and variance σ^2 is denoted as $\mathcal{N}(\mu,\sigma^2)$. $\mathbb{E}\{\bullet\}$ and $\mathsf{cov}\{\bullet,*\} = \mathbb{E}\{(\bullet - \mathbb{E}\{*\})(\bullet - \mathbb{E}\{*\})^\top\}$ denote the expectation and covariance operators, respectively, with $\mathsf{cov}\{\bullet\} = \mathsf{cov}\{\bullet,\bullet\}$. The identity matrix of dimensions $n \times n$ is denoted as $\mathbf{I}_n$. $\mathsf{tr}(\bullet)$ denotes the trace of a matrix. $\mathbf{A} \succ \mathbf{0}, \mathbf{A} \succeq \mathbf{0}$ means that the matrix $\mathbf{A}$ is positive definite and semi-definite, respectively.

II. Problem Statement

Consider a linear system of interest, described by the following stochastic differential equation (SDE):

$$\mathrm{d}\mathbf{x}(t) = \mathbf{A}\mathbf{x}(t)\mathrm{d}t + \mathbf{B}\mathrm{d}\mathbf{w}(t), \quad t \geq 0 \tag{1}$$

where $\mathbf{A} \in \mathbb{R}^{n_\mathbf{x}\times n_\mathbf{x}}$, $\mathbf{B} \in \mathbb{R}^{n_\mathbf{x}\times n_\mathbf{w}}$, and $\mathbf{w}(t)$ is an $n_\mathbf{w}$-dimensional Wiener process with covariance $\mathsf{cov}\{\mathbf{w}(s),\mathbf{w}(r)\} = \mathbf{W}\min(s,r)$ and $\mathbf{W} \succ \mathbf{0}$. As usual, $\mathbf{w}(t)$ is used to model the presence of uncertainty, which can be due to unknown inputs, disturbances, or nonmodeled dynamics [25, Sec. 3.1]. Since this work focuses on observer design, we do not make any assumptions on this disturbance being matched or unmatched. We assume that $\mathbf{x}(0)$ follows a normal distribution with mean $\mathbf{x}_0$ and covariance $\mathbf{P}_0$.

We are interested in estimating $\mathbf{x}(t)$ using a remote estimator, which receives noisy measurements $\mathbf{y}(t) = \mathbf{C}\mathbf{x}(t) + \mathbf{v}(t)$ of the plant from a sensor at some instants $\{t_k\}_{k=0}^{\infty}$, with constant $\mathbf{C} \in \mathbb{R}^{n_\mathbf{y}\times n_\mathbf{x}}$ and $\mathbf{v}(t)$ modeling the measurement noise.

As shown in Fig. 1, the measurements are transmitted over a communication network, which can be shared by other elements. Hence, maintaining a low rate of transmissions is desired. Thus, the sensor uses a deterministic event-triggering condition to decide whether a measurement should be communicated. When the condition is fulfilled, an event is triggered and the measurement is sent to the estimator. We consider no delays in the transmission process. The estimates computed by the remote estimator are used downstream by a controller or monitoring system, which can ask for information about the state of the plant at any arbitrary instant $t \geq 0$.

The goal is to create an EBSE and DETM combination that reduces network transmissions while maintaining a satisfactory remote estimator performance. We aim to prevent estimation uncertainty divergence as the time between events increases. To achieve this, we consider the implicit information obtained from not triggering an event, referred to as *negative*

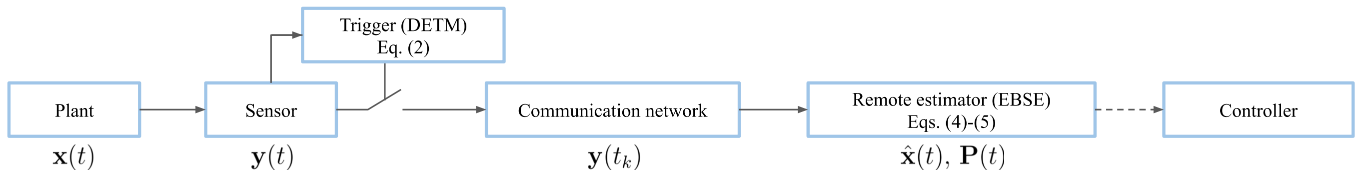

Fig. 1. Problem setup. A sensor measures the output of the plant. A trigger is used to decide when to transmit a measurement over a communication network. A remote estimator receives the asynchronous measurements to produce an estimate of the state of the plant, using a hybrid EBSE: discrete measurements are incorporated at event instants, while negative information from the trigger is incorporated continuously at interevent intervals. A controller asks the estimator for estimates at any time.

information in [19]. It provides the estimator with additional information about the measured signal during interevent intervals without requiring additional transmissions.

A. Unsuitability of Existing DETMs

Note that state estimation of stochastic systems requires the computation of a mean estimate, as well as a measure of uncertainty, usually given in terms of a covariance matrix for the estimation error. Unstable systems experience growing uncertainty between measurements without additional information, as we will illustrate in the simulation examples in Section VI. In the case of using event-triggered communication, especially with a DETM which enlarges the intervals without transmissions of measurements, the unknown transmission instants for new measurements result in potentially unbounded uncertainty and poor estimation quality between events. However, DETM works frequently overlook this issue by disregarding stochastic noise in the system.

In this work, we exploit negative information from the triggering condition to improve the estimates between events, achieving a bounded uncertainty. However, existing DETM designs are not suitable for this task. To infer negative information, the remote estimator must be aware of the sensor's triggering condition between events. Note that, in the usual DETMs, the dynamic variable $\eta(t)$ in the triggering condition has dynamics similar to

$$\dot{\eta}(t) = f(t, \eta(t), e(t))$$

for some function f and $e(t) = \|\mathbf{y}(t) - \mathbf{y}(t_k)\|$ representing the difference between the current measurement of the sensor, $\mathbf{y}(t)$, and the value transmitted at last event, $\mathbf{y}(t_k)$ (e.g., the DETM in [14]). This is, the threshold to trigger an event depends on $\eta(t)$, which in turn depends on the current measurement $\mathbf{y}(t)$. Since the remote estimator is not aware of $\mathbf{y}(t)$ during the interevent intervals, it cannot determine the value of $\eta(t)$ between events. This makes the triggering condition unknown from its point of view and renders the use of negative information unfeasible for existing DETMs.

III. Event-Based Remote Estimation

A. Dynamic Event-Triggering Mechanism

We consider that the sensor has access to the measured signal $\mathbf{y}(t) = \mathbf{C}\mathbf{x}(t) + \mathbf{v}(t)$ for all $t \geq 0$, where $\mathbf{v}(t)$ is normally distributed with zero mean and $\mathsf{cov}\{\mathbf{v}(t)\} = \mathbf{R} \succ \mathbf{0}$. However, these measurements can only be transmitted on a discrete basis. In particular, let $\boldsymbol{\tau} = \{t_k\}_{k=0}^{\infty}$ with $t_0 > 0$ be the increasing sequence of event instants in which measurements are sent from the sensor. We choose the sampling instants through a DETM as

$$\begin{aligned} t_{k+1} &= \inf\{t - t_k > \underline{\tau} \;\mid\; \|\mathbf{y}(t) - \mathbf{y}(t_k)\| \geq \sigma\eta(t) + \varepsilon\} \\ \dot{\eta}(t) &= -c_1\eta(t) + c_2 m_k \quad \forall t \in (t_k, t_{k+1}), \quad \eta(t_k) = \eta_0 \\ m_k &= \frac{\|\mathbf{y}(t_k) - \mathbf{y}(t_{k-1})\|}{t_k - t_{k-1}}, \; k > 0. \end{aligned} \tag{2}$$

The parameter $\underline{\tau} > 0$ is introduced as time regularization, which in practice can be set to the minimum sampling step. Given that our triggering condition (2) depends on measurements affected by stochastic noise, this regularization is necessary to guarantee a minimum interevent time, and it is a solution used by several works in the literature (see [11] and the references therein). Otherwise, the Zeno phenomenon may occur, where an infinite number of events are triggered within a finite-time interval [26, Sec. 1.2.3]. The constants $c_1, c_2, \varepsilon > 0$, $\sigma \in [0, 1]$ are design parameters. Including the static parameter ε in the trigger guarantees a minimum nonzero threshold for the events, since the term $\sigma\eta(t)$ can potentially become zero. The variable m_k is initialized to an arbitrary value $m_0 \geq 0$ and $\eta(0)$ to η_0. Resetting $\eta(t)$ to a fixed value $\eta_0 \geq 0$ at event instants is performed for convenience in our analysis, but it is not strictly necessary. This is because the function $\eta(t)$ is designed to be non-negative for all times, as we will later show in Section IV, in Proposition 1.

Note that the proposed DETM (2) incorporates an auxiliary variable $\eta(t)$ with its own additional dynamics, which depend on the evolution of the measurements. Thus, $\eta(t)$ serves to adapt the triggering threshold for transmissions according to the magnitude of the measured signal, reducing communication accordingly. The evolution of the dynamic variable $\eta(t)$ depends on the measured signal's behavior. If the output signal has a steep slope, the triggering threshold increases, resulting in larger interevent intervals and fewer transmissions. This behavior is consistent with typical DETMs [11].

Moreover, the design allows the estimator to infer additional information. For interevent intervals $t \in (t_k, t_{k+1})$, the remote estimator assumes the triggering condition is not met. In particular, (2) provides the following information:

$$\|\mathbf{y}(t) - \mathbf{y}(t_k)\| < \sigma\eta(t) + \varepsilon =: \delta(t) \quad \forall t \in [t_k, t_{k+1}). \tag{3}$$

The negative information that this conveys is that $\mathbf{y}(t)$ lies within the ball $\mathcal{E}_k(t) = \{\mathbf{y}(t) \mid \|\mathbf{y}(t) - \mathbf{y}(t_k)\| < \delta(t)\}$ for $t \in (t_k, t_{k+1})$. Then, we can condition the probability distribution of the random variable $\mathbf{y}(t)$ to the information at time $t \in$

$[t_k, t_{k+1})$ given by the measurements $\mathcal{I}_t = \{\mathbf{y}(t_k) \quad \forall k \in \mathbb{N}_0 : t_k \leq t\}$ and the negative information $\mathcal{I}_t^\delta = \bigcup_{\ell=0}^{k}\{\mathbf{y}(t) \in \mathcal{E}_\ell(t) \quad \forall t \in (t_\ell, t_{\ell+1})\}$.

While the triggering condition (2) is inspired by the DETM from [14], our design allows the estimator to extract negative information from the triggering threshold $\delta(t)$ in (3), since the dynamics of $\eta(t)$ depend only on the transmitted information at events. Therefore, both the sensor and the estimator can compute $\eta(t)$ and $\delta(t)$ at any time, enabling the use of negative information as opposed to existing DETMs (see Section II-A). Thus, our proposed DETM can reduce communication adaptively, as other DETMs in the literature, but it enables the use of negative information to improve the estimation performance between events.

B. Event-Based State Estimator

Due to the nature of the available information, we propose an EBSE with a hybrid update schedule for the remote estimator: a continuous correction is performed by including negative information at interevent intervals, while discrete jumps occur at events generated as a consequence of a new transmitted measurement.

The motivation for the estimator design is that, at interevent intervals $t \in (t_k, t_{k+1})$, the difference $\mathbf{y}(t) - \mathbf{y}(t_k)$ in (3) can be overestimated by a Gaussian noise with zero mean and covariance $\mathbf{E}(t) = \delta(t)^2\mathbf{I}_{n_\mathbf{y}}$. Then, using this approximation, we can consider that there is an implicit measurement at $t \in (t_k, t_{k+1})$ given by $\mathbf{y}(t_k)$, with an additional covariance term $\mathbf{E}(t)$ modeling the amount of noise introduced by the difference $\mathbf{y}(t) - \mathbf{y}(t_k)$. We propose to incorporate this information as follows during $t \in [t_k, t_{k+1})$:

$$\mathbf{E}(t) = (\sigma\eta(t) + \varepsilon)^2\mathbf{I}_{n_\mathbf{y}}, \quad \mathbf{M}(t) = \mathbf{R} + \mathbf{E}(t) \tag{4a}$$

$$\mathbf{G}(t) = \mathbf{P}(t)\mathbf{C}^\top\mathbf{M}(t)^{-1} \tag{4b}$$

$$\frac{\mathrm{d}\hat{\mathbf{x}}(t)}{\mathrm{d}t} = \mathbf{A}\hat{\mathbf{x}}(t) + \mathbf{G}(t)(\mathbf{y}(t_k) - \mathbf{C}\hat{\mathbf{x}}(t)) \tag{4c}$$

$$\frac{\mathrm{d}\mathbf{P}(t)}{\mathrm{d}t} = \mathbf{A}\mathbf{P}(t) + \mathbf{P}(t)\mathbf{A}^\top + \mathbf{B}\mathbf{W}\mathbf{B}^\top - \mathbf{G}(t)\mathbf{M}(t)\mathbf{G}(t)^\top \tag{4d}$$

and under initial conditions $\hat{\mathbf{x}}(t_k), \mathbf{P}(t_k)$ for such interval. In (4), $\mathbf{M}(t)$ represents the noise covariance of the implicit measurement between events, and $\mathbf{G}(t)$ is the gain for the continuous update of the estimator.

At an event time t_k, the estimate $\hat{\mathbf{x}}(t_k)$ can be obtained by correcting the estimate $\hat{\mathbf{x}}(t)$ from (4) prior to receiving $\mathbf{y}(t_k)$, which we denote as $\hat{\mathbf{x}}(t_k^-) := \lim_{t\to t_k^-}\hat{\mathbf{x}}(t)$ and $\mathbf{P}(t_k^-) := \lim_{t\to t_k^-}\mathbf{P}(t)$

$$\begin{aligned}\mathbf{L}(t_k) &= \mathbf{P}(t_k^-)\mathbf{C}^\top\left(\mathbf{C}\mathbf{P}(t_k^-)\mathbf{C}^\top + \mathbf{R}\right)^{-1}\\ \hat{\mathbf{x}}(t_k) &= \hat{\mathbf{x}}(t_k^-) + \mathbf{L}(t_k)\big(\mathbf{y}(t_k) - \mathbf{C}\hat{\mathbf{x}}(t_k^-)\big)\\ \mathbf{P}(t_k) &= \big(\mathbf{I}_{n_\mathbf{x}} - \mathbf{L}(t_k)\mathbf{C}\big)\mathbf{P}(t_k^-)\end{aligned} \tag{5}$$

where $\mathbf{L}(t_k)$ is the gain for the discrete event update. For completeness, define $\hat{\mathbf{x}}(t_0^-) := \mathbf{x}_0$ and $\mathbf{P}(t_0^-) := \mathbf{P}_0$.

Note that the proposed EBSE incorporates the measurements received at events similarly to a Kalman filter, as in (5). However, between events, event-triggered Kalman filters often use a model-based prediction to fill the gap without new sensor information. In contrast, we propose the update (4), which resembles a Kalman–Bucy filter but uses the implicit measurement from negative information during $t \in (t_k, t_{k+1})$ rather than the real measurement $\mathbf{y}(t)$, which is unknown to the estimator. This update using negative information between events aims to improve estimation performance at these intervals, without requiring further transmissions of information.

Our EBSE builds on the idea presented in [19] of incorporating negative information, but we have introduced two main differences in our proposal. First, [19] assumes that a synchronous controller uses the state estimates and decides to incorporate negative information only at synchronous instants, even though the measured signal is continuous, and thus negative information is also available between sampling instants of the controller. In contrast, due to our hybrid approach, we incorporate negative information continuously between events. This is, we take advantage of all available information at interevent intervals, not just at synchronous instants, and we obtain estimates for all time, regardless of the sampling frequency of a downstream element. Second, in [19], negative information is included as an ellipsoidal outer bound, while we use a Gaussian process to overestimate negative information. This approach yields less conservative results, as we show in Section VI.

IV. Main Results

Now, we show the main results derived from our EBSE and DETM proposal. First, we establish some important guarantees of our DETM.

Proposition 1: Consider the event-triggering rule (2). Then, the resulting sequence of event instants $\boldsymbol{\tau}$ does not exhibit Zeno behavior. Moreover, $0 \leq \eta(t) \leq \max\{\eta_0, c_\eta\bar{\eta}_k\} \quad \forall t \in [t_k, t_{k+1})$, where

$$c_\eta = \frac{c_2\nu_{\max}(t_k)}{c_1\underline{\tau}}, \quad \nu_{\max}(t_k) = \sqrt{\max\{\mathbf{D}(t_k)_{ii}\}}$$

and $\bar{\eta}_k$ is distributed as $\chi(n_\mathbf{y}, \lambda_k)$ with

$$\begin{aligned}\lambda_k &= \sqrt{\boldsymbol{\mu}(t_k)^\top\mathbf{D}(t_k)^{-1}\boldsymbol{\mu}(t_k)}\\ \boldsymbol{\mu}(t_k) &= \mathbf{H}(t_k)^\top\mathbf{C}\big(\mathbf{A}_\mathsf{d}(\Delta_k) - \mathbf{I}_{n_\mathbf{x}}\big)\hat{\mathbf{x}}^*(t_{k-1})\end{aligned}$$

where $\hat{\mathbf{x}}^*(t_{k-1}) = \mathbb{E}\{\mathbf{x}(t_{k-1}) \mid \mathcal{I}_{t_{k-1}}\}$, defining $\Delta_k = t_k - t_{k-1}$, $\mathbf{A}_\mathsf{d}(\Delta_k) = \exp(\mathbf{A}\Delta_k))$ and

$$\mathbf{W}_\mathsf{d}(\Delta_k) = \int_0^{\Delta_k}\mathbf{A}_\mathsf{d}(\tau)\mathbf{B}\mathbf{W}\mathbf{B}^\top\mathbf{A}_\mathsf{d}(\tau)^\top\mathrm{d}\tau.$$

Then, the matrices $\mathbf{D}(t_k)$, $\mathbf{H}(t_k)$, which depend on $\mathbf{P}^*(t_{k-1}) = \mathsf{cov}\{\mathbf{x}(t_{k-1}) - \hat{\mathbf{x}}(t_{k-1}) \mid \mathcal{I}_{t_{k-1}}\}$, are defined from the spectral decomposition $\mathbf{S}(t_k) = \mathbf{H}(t_k)\mathbf{D}(t_k)\mathbf{H}(t_k)^\top$, with

$$\begin{aligned}\mathbf{S}(t_k) = \mathbf{C}\big(\mathbf{A}_\mathsf{d}(\Delta_k) - \mathbf{I}_{n_\mathbf{x}}\big)\mathbf{P}^*(t_{k-1})\big(\mathbf{A}_\mathsf{d}(\Delta_k) - \mathbf{I}_{n_\mathbf{x}}\big)^\top\mathbf{C}^\top\\ + \mathbf{C}\mathbf{W}_\mathsf{d}(\Delta_k)\mathbf{C}^\top + 2\mathbf{R}.\end{aligned}$$

Proof: First, we prove the absence of Zeno behavior due to the triggering mechanism. Note that, by design, the interevent intervals always fulfill the condition $\Delta_k := t_k - t_{k-1} \geq \underline{\tau}$. Thus, $t_k \geq t_0 + k\underline{\tau}$ and $\lim_{k\to\infty} t_k \geq \lim_{k\to\infty} t_0 + k\underline{\tau} = \infty$. This means that an infinite number of events cannot be triggered in a finite amount of time, excluding Zeno behavior.

For the rest of the proposition, the evolution of $\eta(t)$ for $t \in [t_k, t_{k+1})$ is explicitly given by

$$\eta(t) = \frac{c_2}{c_1} m_k \left(1 - e^{-c_1(t-t_k)}\right) + \eta_0 e^{-c_1(t-t_k)}.$$

Hence, $\eta(t)$ evolves monotonically from η_0 to an asymptotic value of $c_2 m_k / c_1$, where $\eta_0 \geq 0$, $c_1, c_2 > 0$ and $m_k \geq 0$ due to its definition (2). This leads to

$$0 \leq \min\{\eta_0, c_2 m_k / c_1\} \leq \eta(t) \leq \max\{\eta_0, c_2 m_k / c_1\}.$$

Now, we provide a bound for $c_2 m_k / c_1$ as

$$\frac{c_2 m_k}{c_1} \leq \frac{c_2}{c_1 \underline{\tau}} \|\mathbf{y}(t_k) - \mathbf{y}(t_{k-1})\| \tag{6}$$

where we used $1/\Delta_k \leq 1/\underline{\tau}$.

Note that the sampled-data equivalent of (1) at the discrete-time event instants $t \in \{t_k\}_{k=0}^{\infty}$ is given by [25, Sec. 4.5.2]

$$\mathbf{x}(t_k) = \mathbf{A}_\mathsf{d}(\Delta_k)\mathbf{x}(t_{k-1}) + \mathbf{w}_\mathsf{d}(t_{k-1})$$

where $\mathbf{w}_\mathsf{d}(t_{k-1})$ is normally distributed with zero mean and covariance $\mathbf{W}_\mathsf{d}(\Delta_k)$.

Using the above, let $\tilde{\mathbf{y}}(t_k) = \mathbf{y}(t_k) - \mathbf{y}(t_{k-1})$, which can be written as

$$\begin{aligned}\tilde{\mathbf{y}}(t_k) &= \mathbf{C}\mathbf{x}(t_k) + \mathbf{v}(t_k) - \mathbf{C}\mathbf{x}(t_{k-1}) - \mathbf{v}(t_{k-1}) \\ &= \mathbf{C}(\mathbf{A}_\mathsf{d}(\Delta_k)\mathbf{x}(t_{k-1}) + \mathbf{w}_\mathsf{d}(t_{k-1})) + \mathbf{v}(t_k) \\ &\quad - \mathbf{C}\mathbf{x}(t_{k-1}) - \mathbf{v}(t_{k-1}) \\ &= \mathbf{C}\big(\mathbf{A}_\mathsf{d}(\Delta_k) - \mathbf{I}_{n_\mathbf{x}}\big)\mathbf{x}(t_{k-1}) + \mathbf{C}\mathbf{w}_\mathsf{d}(t_{k-1}) + \tilde{\mathbf{v}}(t_k)\end{aligned} \tag{7}$$

with $\tilde{\mathbf{v}}(t_k) = \mathbf{v}(t_k) - \mathbf{v}(t_{k-1})$. Now, note that

$$\begin{aligned}&\mathsf{cov}\Big\{\mathbf{C}\big(\mathbf{A}_\mathsf{d}(\Delta_k) - \mathbf{I}_{n_\mathbf{x}}\big)\mathbf{x}(t_{k-1})\Big\} \\ &= \mathbf{C}\big(\mathbf{A}_\mathsf{d}(\Delta_k) - \mathbf{I}_{n_\mathbf{x}}\big)\mathsf{cov}\{\mathbf{x}(t_{k-1})\}\big(\mathbf{A}_\mathsf{d}(\Delta_k) - \mathbf{I}_{n_\mathbf{x}}\big)^\top \mathbf{C}^\top \\ &= \mathbf{C}\big(\mathbf{A}_\mathsf{d}(\Delta_k) - \mathbf{I}_{n_\mathbf{x}}\big)\mathbf{P}^*(t_{k-1})\big(\mathbf{A}_\mathsf{d}(\Delta_k) - \mathbf{I}_{n_\mathbf{x}}\big)^\top \mathbf{C}^\top\end{aligned}$$

where we have used that the covariance of $\mathbf{x}(t_{k-1})$ conditioned on the measurements that are received up to t_{k-1}, i.e., $\mathcal{I}_{t_{k-1}}$, is $\mathbf{P}^*(t_{k-1})$ [27, Sec. 3.1]. Note that we can still write that $\mathbf{x}(t_k) = \mathbf{A}_\mathsf{d}(\Delta_k)\mathbf{x}(t_{k-1}) + \mathbf{w}_\mathsf{d}(t_{k-1})$ as we had done in (7), since we are not conditioning to $\mathbf{y}(t_k)$. In addition, $\mathsf{cov}\{\mathbf{C}\mathbf{w}_\mathsf{d}(t_{k-1})\} = \mathbf{C}\mathsf{cov}\{\mathbf{w}_\mathsf{d}(t_{k-1})\}\mathbf{C}^\top = \mathbf{C}\mathbf{W}_\mathsf{d}(\Delta_k)\mathbf{C}^\top$ and $\mathsf{cov}\{\tilde{\mathbf{v}}(t_k)\} = 2\mathbf{R}$, due to $\mathbf{v}(t_k)$ and $\mathbf{v}(t_{k-1})$ being independent. Since the three terms of $\tilde{\mathbf{y}}(t_k)$ in (7) are also independent Gaussians, we have

$$\begin{aligned}\mathsf{cov}\{\tilde{\mathbf{y}}(t_k)\} &= \mathbf{C}\big(\mathbf{A}_\mathsf{d}(\Delta_k) - \mathbf{I}_{n_\mathbf{x}}\big)\mathbf{P}^*(t_{k-1}) \\ &\quad \times \big(\mathbf{A}_\mathsf{d}(\Delta_k) - \mathbf{I}_{n_\mathbf{x}}\big)^\top \mathbf{C}^\top + \mathbf{C}\mathbf{W}_\mathsf{d}(\Delta_k)\mathbf{C}^\top + 2\mathbf{R}.\end{aligned}$$

The covariance is a real symmetric matrix, for which we can apply the standard spectral decomposition, yielding $\mathsf{cov}\{\tilde{\mathbf{y}}(t_k)\} = \mathbf{S}(t_k) = \mathbf{H}(t_k)\mathbf{D}(t_k)\mathbf{H}(t_k)^\top$ where $\mathbf{D}(t_k)$ is a diagonal matrix containing the eigenvalues of $\mathsf{cov}\{\tilde{\mathbf{y}}(t_k)\}$ and $\mathbf{H}(t_k)$ is orthogonal. Then, define $\mathbf{z}(t_k) := \mathbf{H}(t_k)^\top \tilde{\mathbf{y}}(t_k)$, which has $\|\mathbf{z}(t_k)\|^2 = \|\tilde{\mathbf{y}}(t_k)\|^2$, and $\mathsf{cov}\{\mathbf{z}(t_k)\} = \mathbf{D}(t_k)$. The square root of the sum of the squares of k-independent normal variables $\mathcal{N}(0, 1)$ follows a chi distribution with k degrees of freedom. In our case, $\mathbf{z}(t_k)$ follows a normal distribution since it is a linear transformation of $\tilde{\mathbf{y}}(t_k)$, which is Gaussian. Additionally, the covariance of $\mathbf{z}(t_k)$ is given by the diagonal matrix $\mathbf{D}(t_k)$, meaning that the elements of $\mathbf{z}(t_k)$ are uncorrelated. This, along with the fact that the elements of $\mathbf{z}(t_k)$ are jointly Gaussian, implies that they are also independent [25, p. 12]. Then, we can define a random variable $\bar{\eta}_k$ which follows a chi distribution with $n_\mathbf{y}$ degrees of freedom and noncentrality parameter λ_k, with

$$\bar{\eta}_k = \sqrt{\mathbf{z}(t_k)^\top \mathbf{D}(t_k)^{-1}\mathbf{z}(t_k)}, \quad \lambda_k = \sqrt{\boldsymbol{\mu}(t_k)^\top \mathbf{D}(t_k)^{-1}\boldsymbol{\mu}(t_k)} \tag{8}$$

where $\boldsymbol{\mu}(t_k)$ is the expected value of $\mathbf{z}(t_k)$ at $t = t_k$, conditioned to the measurements received before that time. By virtue of $\mathbb{E}\{\mathbf{v}(t_k)\} = 0$, $\mathbb{E}\{\mathbf{w}_\mathsf{d}(t_k)\} = 0$, and $\mathbb{E}\{\mathbf{x}(t_{k-1})|\mathcal{I}_{t_{k-1}}\} = \hat{\mathbf{x}}^*(t_{k-1})$, we have that [27, Sec. 3.1]

$$\begin{aligned}\boldsymbol{\mu}(t_k) &= \mathbb{E}\Big\{\mathbf{H}(t_k)^\top \tilde{\mathbf{y}}(t_k)|\mathbf{y}(0), \ldots, \mathbf{y}(t_{k-1})\Big\} \\ &= \mathbf{H}(t_k)^\top \mathbf{C}\big(\mathbf{A}_\mathsf{d}(\Delta_k) - \mathbf{I}_{n_\mathbf{x}}\big)\hat{\mathbf{x}}^*(t_{k-1}).\end{aligned}$$

Recalling that $\|\tilde{\mathbf{y}}(t_k)\| = \|\mathbf{H}(t_k)^\top \tilde{\mathbf{y}}(t_k)\| = \|\mathbf{z}(t_k)\|$ due to $\mathbf{H}(t_k)$ being orthogonal, we have

$$\begin{aligned}\|\tilde{\mathbf{y}}(t_k)\| &= \|\mathbf{z}(t_k)\| = \sqrt{\mathbf{z}(t_k)^\top \mathbf{z}(t_k)} \\ &= \sqrt{\mathbf{z}(t_k)^\top \mathbf{D}(t_k)^{-1}\mathbf{D}(t_k)\mathbf{z}(t_k)}\end{aligned}$$

where we have introduced the identity term $\mathbf{D}(t_k)^{-1}\mathbf{D}(t_k)$. Then, using the definition of $\bar{\eta}_k$ from (8) and the fact that $\|\mathbf{D}(t_k)\| \leq \max\{\mathbf{D}(t_k)_{ii}\}$, where $\max\{\mathbf{D}(t_k)_{ii}\}$ is the largest eigenvalue of $\mathbf{D}(t_k)$ due to it being a diagonal matrix, we reach

$$\|\tilde{\mathbf{y}}(t_k)\| \leq \nu_{\max}(t_k)\bar{\eta}_k \tag{9}$$

with $\nu_{\max}(t_k) = \sqrt{\max\{\mathbf{D}(t_k)_{ii}\}}$. Using (9) in (6) leads to

$$\frac{c_2 m_k}{c_1} \leq \frac{c_2 \nu_{\max}(t_k)}{c_1 \underline{\tau}} \bar{\eta}_k = c_\eta \bar{\eta}_k$$

which completes the proof. ∎

In the following results, we establish some desirable properties complied by the EBSE in (4) and (5). Before stating the main theorem of this work, we first show some technical lemmas.

Consider the following artifact system composed by the SDE in (1) along with the hybrid measurements:

$$\begin{aligned}\mathbf{y}(t) &= \mathbf{C}\mathbf{x}(t) + \mathbf{v}(t), \quad t \in \boldsymbol{\tau} = \{t_k\}_{k=0}^{\infty} \\ \mathbf{y}'(t) &= \mathbf{C}\mathbf{x}(t) + \mathbf{v}'(t), \quad t \notin \boldsymbol{\tau} = \{t_k\}_{k=0}^{\infty}\end{aligned} \tag{10}$$

where $\mathsf{cov}\{\mathbf{v}(t_k)\} = \mathbf{R}$ and $\mathsf{cov}\{\mathbf{v}'(t)\} = \mathbf{M}(t) \quad \forall t \in (t_k, t_{k+1})$ with $\mathbf{M}(t)$ as in (4). Moreover, define the sets of causal measurements until an instant T as $\mathcal{I}_T = \{\mathbf{y}(t_k) \quad \forall k \in \mathbb{N}_0 : t_k \leq T\}$, $\mathcal{I}'_T = \{\mathbf{y}'(t) \quad \forall t \in [0, T] : t \notin \boldsymbol{\tau}\}$. Additionally, consider the following assumptions.

Assumption 1 [28]: Define the matrices

$$\begin{aligned}\mathbf{M}_o(t_0, t) &= \int_{t_0}^{t} \mathbf{A}_\mathsf{d}(\tau - t)^\top \mathbf{C}^\top \mathbf{C}\mathbf{A}_\mathsf{d}(\tau - t)\mathrm{d}\tau \\ \mathbf{M}_c(t_0, t) &= \int_{t_0}^{t} \mathbf{A}_\mathsf{d}(t - \tau)\mathbf{B}\mathbf{B}^\top \mathbf{A}_\mathsf{d}(t - \tau)^\top \mathrm{d}\tau.\end{aligned}$$

The pairs $(\mathbf{A}, \mathbf{C})$ and $(\mathbf{A}, \mathbf{B})$ are uniformly completely observable (UCO) and uniformly completely controllable (UCC), meaning that there exist fixed constants $\underline{\alpha}_o, \overline{\alpha}_o, \sigma_o > 0$ and $\underline{\alpha}_c, \overline{\alpha}_c, \sigma_c > 0$ such that for all time:

$$\underline{\alpha}_o \mathbf{I}_{n_\mathbf{x}} \preceq \mathbf{M}_o(t-\sigma_o, t) \preceq \overline{\alpha}_o \mathbf{I}_{n_\mathbf{x}}$$
$$\underline{\alpha}_c \mathbf{I}_{n_\mathbf{x}} \preceq \mathbf{M}_c(t-\sigma_c, t) \preceq \overline{\alpha}_c \mathbf{I}_{n_\mathbf{x}}.$$

Assumption 2: Given the measurement sequence $\{\mathbf{v}(t)\}_{t\geq 0}$, there exists $\overline{\alpha}_m > 0$ such that $\|\mathbf{M}(t)\| \leq \overline{\alpha}_m \quad \forall t \geq 0$.

Remark 1: Assumption 1 is commonly required in observer design, particularly in relation to Kalman filtering. Assumption 2 is complied almost surely as a result of Proposition 1. To verify this, recall that $\mathbf{M}(t) = \mathbf{R} + \mathbf{E}(t)$, where $\mathbf{R}$ is constant and $\mathbf{E}(t)$ depends on $\eta(t)$. Furthermore, $\eta(t)$ evolves with the sequence of measurements and therefore has a deterministic evolution when considering a certain realization of $\{\mathbf{v}(t)\}_{t\geq 0}$. Proposition 1 implies that for any $t \geq 0$, $\lim_{\eta_{\max}\to\infty} \mathbb{P}(\eta(t) \geq \eta_{\max}) = 0$, i.e., there exists $\eta_{\max}$ such that $\eta(t) \leq \eta_{\max} \quad \forall t \geq 0$ almost surely, from which uniform boundedness of $\|\mathbf{M}(t)\|$ follows.

Lemma 1: Consider the system (1) along with the measurements (10). Then, the optimal estimate $\hat{\mathbf{x}}(t) = argmin_{\hat{\mathbf{x}}\in\mathbb{R}^{n_\mathbf{x}}} \mathrm{tr}(\mathbf{P}(t))$ with $\mathbf{P}(t) := \mathrm{cov}\{\mathbf{x}(t) - \hat{\mathbf{x}}(t) \mid \mathcal{I}_t, \mathcal{I}'_t\}$ satisfies (4) and (5).

Proof: We prove Lemma 1 by induction. We start at an event instant t_{k-1}, for which an optimal estimate is available; then, we proceed to show optimality of the estimates from (4) for the interval (t_{k-1}, t_k), and finally we show that the update in (5) yields the optimal estimate at the next event t_k, completing the recursion. First, assume that $\hat{\mathbf{x}}(t_{k-1})$ is the optimal estimate of $\mathbf{x}(t_{k-1})$ in the sense that it minimizes $\mathrm{tr}(\mathbf{P}(t_{k-1})) = \mathrm{cov}\{\mathbf{x}(t_{k-1}) - \hat{\mathbf{x}}(t_{k-1}) \mid \mathcal{I}_{t_{k-1}}, \mathcal{I}'_{t_{k-1}}\}$. For the interval $t \in (t_{k-1}, t_k)$ the only new information comes from the measurements $\mathbf{y}'(t) \in \mathcal{I}'_t$, which are incorporated to the estimates as in (4) with $\mathbf{y}'(t)$ instead of $\mathbf{y}(t_{k-1})$. Note that (4) acts as a Kalman–Bucy filter during (t_{k-1}, t_k) since no events occur in such interval by construction. Optimality for this kind of filter is established in [28, Th. 1]. Therefore, the estimates $\hat{\mathbf{x}}(t)$, $\mathbf{P}(t)$ computed from (4) under these conditions are optimal, with $\mathbf{P}(t) = \mathrm{cov}\{\mathbf{x}(t) - \hat{\mathbf{x}}(t) \mid \mathcal{I}_t, \mathcal{I}'_t\}$. At $t = t_k$, two pieces of information are available: the new measurement $\mathbf{y}(t_k) \in \mathcal{I}_{t_k}$, and the estimate $\hat{\mathbf{x}}(t_k^-) = \lim_{t\to t_k^-} \hat{\mathbf{x}}(t)$ from (4), which can be considered the a priori estimate taking into account all the previously available information before including the new $\mathbf{y}(t_k)$. Then, considering the expression for $\hat{\mathbf{x}}(t_k)$ as in (5), the optimal a posteriori covariance matrix $\mathbf{P}(t_k) = \mathrm{cov}\{\mathbf{x}(t_k) - \hat{\mathbf{x}}(t_k) \mid \mathcal{I}_{t_k}, \mathcal{I}'_{t_k}\}$ and the optimal gain $\mathbf{L}(t_k)$ can be derived such that $\mathrm{tr}(\mathbf{P}(t_k))$ is minimized, following similar steps as for the Kalman filter shown in [29]. We start by expanding the expression of $\mathbf{P}(t_k)$ by substituting $\hat{\mathbf{x}}(t_k)$ from (5), using $\mathbf{y}(t_k) = \mathbf{C}\mathbf{x}(t_k) + \mathbf{v}(t_k)$ and $\mathbf{P}(t_k^-) = \mathrm{cov}\{\mathbf{x}(t_k^-) - \hat{\mathbf{x}}(t_k^-)\}$

$$\begin{aligned}
\mathbf{P}(t_k) &= \mathrm{cov}\left\{\mathbf{x}(t_k) - \hat{\mathbf{x}}\left(t_k^-\right) - \mathbf{L}(t_k)\left(\mathbf{y}(t_k) - \mathbf{C}\hat{\mathbf{x}}\left(t_k^-\right)\right)\right\} \\
&= \mathrm{cov}\left\{(\mathbf{I} - \mathbf{L}(t_k)\mathbf{C})\left(\mathbf{x}(t_k) - \hat{\mathbf{x}}\left(t_k^-\right)\right) - \mathbf{L}(t_k)\mathbf{v}(t_k)\right\} \\
&= (\mathbf{I} - \mathbf{L}(t_k)\mathbf{C})\mathbf{P}(t_k^-)(\mathbf{I} - \mathbf{L}(t_k)\mathbf{C})^\top + \mathbf{L}(t_k)\mathbf{R}\mathbf{L}(t_k)^\top.
\end{aligned}$$

Rearranging, the expression above can be rewritten as

$$\begin{aligned}
\mathbf{P}(t_k) = \mathbf{P}\left(t_k^-\right) - \mathbf{L}(t_k)\mathbf{C}\mathbf{P}\left(t_k^-\right) - \mathbf{P}\left(t_k^-\right)\mathbf{C}^\top\mathbf{L}(t_k)^\top \\
+ \mathbf{L}(t_k)\mathbf{S}(t_k)\mathbf{L}(t_k)^\top
\end{aligned}$$

where $\mathbf{S}(t_k) = \mathbf{C}\mathbf{P}(t_k^-)\mathbf{C}^\top + \mathbf{R}$. Then, the optimal gain $\mathbf{L}(t_k)$ can be derived to minimize the trace of $\mathbf{P}(t_k)$. The derivative of the trace, i.e., the gradient of $\mathrm{tr}(\mathbf{P}(t_k))$ with respect to the components of $\mathbf{L}(t_k)$, yields $\partial\mathrm{tr}(\mathbf{P}(t_k))/\partial\mathbf{L}(t_k) = -2(\mathbf{C}\mathbf{P}(t_k^-))^\top + 2\mathbf{L}(t_k)\mathbf{S}(t_k)$. Hence, setting $\partial\mathrm{tr}(\mathbf{P}(t_k))/\partial\mathbf{L}(t_k) = \mathbf{0}$, we have that

$$\mathbf{L}(t_k) = \mathbf{P}\left(t_k^-\right)\mathbf{C}^\top\mathbf{S}(t_k)^{-1} = \mathbf{P}\left(t_k^-\right)\mathbf{C}^\top\left(\mathbf{C}\mathbf{P}\left(t_k^-\right)\mathbf{C}^\top + \mathbf{R}\right)^{-1}$$

which matches the gain in (5). The expression for $\mathbf{P}(t_k)$ can then be simplified to the one in (5). Finally, the recursion is completed by noting that the initial conditions $\hat{\mathbf{x}}(t_0^-), \mathbf{P}(t_0^-)$ defined after (5) lead to optimal $\hat{\mathbf{x}}(t_0), \mathbf{P}(t_0)$ by the same argument as before. ■

Lemma 2: Let Assumptions 1 and 2 hold. Let $\hat{\mathbf{x}}'(t), \mathbf{P}'(t)$ satisfy (4), with (4c) substituted by

$$\frac{\mathrm{d}\hat{\mathbf{x}}(t)}{\mathrm{d}t} = \mathbf{A}\hat{\mathbf{x}}(t) + \mathbf{G}(t)\left(\mathbf{y}'(t) - \mathbf{C}\hat{\mathbf{x}}(t)\right)$$

along with $\mathbf{y}'(t)$ defined in (10), as well as $\hat{\mathbf{x}}'(t_k^-) = \lim_{t\to t_k^-} \hat{\mathbf{x}}'(t), \mathbf{P}'(t_k^-) = \lim_{t\to t_k^-} \mathbf{P}'(t)$. Then, $\mathbf{P}'(t) := \mathrm{cov}\{\mathbf{x}(t) - \hat{\mathbf{x}}'(t) \mid \mathcal{I}'_t\}$ and $\mathrm{tr}(\mathbf{P}'(t))$ is uniformly bounded $\forall t \geq 0$.

Proof: First note that the definitions of $\hat{\mathbf{x}}'(t), \mathbf{P}'(t)$ correspond to the trajectories of a Kalman–Bucy filter using only information in $\mathcal{I}'_t$ with $\mathbf{P}'(t) := \mathrm{cov}\{\mathbf{x}(t) - \hat{\mathbf{x}}'(t) \mid \mathcal{I}'_t\}$. Note that the filter using only these measurements is no longer event-triggered since it uses the continuous measurements in $\mathcal{I}'_t$ but skips the discrete event update (5). Given that the measurements $\mathbf{y}'(t)$ are Gaussian, we analyze the estimator using the same arguments as in [28]. In particular, [28, Th. 4] can be used to conclude boundedness of $\mathrm{tr}(\mathbf{P}'(t))$, since the following properties are complied: 1) the system is UCO and UCC by Assumption 1; 2) the existence of constants $\alpha_a, \underline{\alpha}_w, \bar{\alpha}_w > 0$ such that $\underline{\alpha}_w \leq \|\mathbf{W}\| \leq \bar{\alpha}_w, \|\mathbf{A}\| \leq \alpha_a$ due to $\mathbf{W} \succ 0, \mathbf{A}$ being constant matrices; and 3) the existence of $\underline{\alpha}_m, \bar{\alpha}_m > 0$ such that $\underline{\alpha}_m \leq \|\mathbf{M}(t)\| \leq \bar{\alpha}_m$ is ensured by Assumption 2 and since $\mathbf{M}(t) \succeq \mathbf{R} + \varepsilon^2\mathbf{I}_{n_\mathbf{y}}$. ■

Now, we are ready to show the main result of our EBSE.

Theorem 3: Let Assumptions 1 and 2 hold. Consider the EBSE in (4) and (5) in the remote estimator as well as the ETM in (2). Then, the following are complied.

1) *Boundedness:* $\mathrm{tr}(\mathbf{P}(t))$ is uniformly bounded $\forall t \geq 0$, regardless of $\{t_k\}_{k=0}^\infty$.
2) *Consistency:* $\mathrm{cov}\{\mathbf{x}(t) - \hat{\mathbf{x}}(t)\} \preceq \mathbf{P}(t)$.
3) *Interevent Asymptotic Solution:* Assuming $(t_{k+1} - t_k) \to \infty$ then $\lim_{t-t_k\to\infty} \mathbf{P}(t) = \mathbf{P}_\infty$ where $\mathbf{P}_\infty$ is the solution to

$$\mathbf{A}\mathbf{P}_\infty + \mathbf{P}_\infty\mathbf{A}^\top + \mathbf{B}\mathbf{W}\mathbf{B}^\top - \mathbf{P}_\infty\mathbf{C}^\top\mathbf{M}_k^{-1}\mathbf{C}\mathbf{P}_\infty = \mathbf{0} \tag{11}$$

with

$$\mathbf{M}_k = \left(\sigma\frac{c_2}{c_1}m_k + \varepsilon\right)^2\mathbf{I}_{n_\mathbf{y}} + \mathbf{R}. \tag{12}$$

Proof: Item 1): Note that since $\hat{\mathbf{x}}(t)$ is optimal for $\mathrm{tr}(\mathbf{P}(t))$ as a result of Lemma 1 then $\mathrm{tr}(\mathbf{P}(t)) \leq \mathrm{tr}(\mathbf{P}'(t))$ for $\mathbf{P}'(t)$ given in Lemma 2. Finally, boundedness of $\mathrm{tr}(\mathbf{P}'(t))$ from Lemma 2 implies the same conclusion for $\mathrm{tr}(\mathbf{P}(t))$, completing the proof for this item.

Item 2): Our EBSE is conservative since the negative information is modeled as an over-estimated Gaussian process around the last measurement. Formally, note that by construction $\mathbf{y}(t_k) = \mathbf{y}(t) + \mathbf{v}^\delta(t) = \mathbf{C}\mathbf{x}(t) + \mathbf{v}(t) + \mathbf{v}^\delta(t) \quad \forall t \in [t_k, t_{k+1})$ with $\|\mathbf{v}^\delta(t)\| \le \delta(t) = \sigma\eta(t) + \varepsilon$ as a consequence of (3). Now, denote the components $\mathbf{v}^\delta(t) = [v_1^\delta(t), \ldots, v_{n_\mathrm{y}}^\delta(t)]^\top$ and note that each $|v_i^\delta(t)| \le \delta(t) \quad \forall i \in \{1, \ldots, n_\mathrm{y}\}$ so that $\mathrm{cov}\{v_i^\delta(t)\} \le \delta(t)^2$ due to Popoviciu's inequality on variances. Assuming $\{v_i(t)\}_{i=1}^{n_\mathrm{y}}$ are noncorrelated, the covariance of the total noise is $\mathrm{cov}\{\mathbf{v}^\delta(t) + \mathbf{v}(t)\} \preceq \delta(t)^2\mathbf{I}_{n_\mathrm{y}} + \mathbf{R} = \mathrm{cov}\{\mathbf{v}'(t)\}$ with $\mathbf{v}'(t)$ defined in (10). Hence, the noise considered in the Kalman–Bucy filter in the proof of Lemma 2 is of bigger magnitude than the actual one from $\mathbf{v}(t) + \mathbf{v}^\delta(t)$. Therefore, this conservativeness along with the conservativeness arising from the assumption of $\mathbf{v}^\delta(t)$ having uncorrelated components leads to conclude that $\mathbf{P}(t)$ from (4) along with (5) is conservative with respect to the true covariance $\mathrm{cov}\{\mathbf{x}(t) - \hat{\mathbf{x}}(t)\}$.

Item 3): First, note that $\eta_k := \lim_{t-t_k\to\infty} \eta(t) = (c_2/c_1)m_k$. Consequently, let $\mathbf{E}_k := \lim_{t-t_k\to\infty} \mathbf{E}(t) = (\sigma\eta_k + \varepsilon)^2\mathbf{I}_{n_\mathrm{y}}$ and $\mathbf{M}_k := \mathbf{E}_k + \mathbf{R}$ as in (12). Note that, as established in the proof of Lemma 2, during $t \in (t_k, t_{k+1})$, (4) is a Kalman–Bucy filter for the information $\mathcal{I}'_t$. For observable systems with bounded matrices $\mathbf{A}, \mathbf{R}, \mathbf{W}$, the Kalman–Bucy filter is uniformly asymptotically stable, and every solution to (4) starting at a $\mathbf{P}(0) \succeq \mathbf{0}$ converges to a limit, which is guaranteed to have a solution for all t given by (11) according to [28]. Now, consider a nominal Kalman–Bucy filter (4) for the linear time-invariant version of system (1) with constant $\mathbf{A}, \mathbf{B}, \mathbf{C}, \mathbf{W}, \mathbf{R}$ and $\mathbf{E}(t)$ replaced by its asymptotic value $\mathbf{E}_k$. For this nominal system, $\lim_{t-t_k\to\infty} \mathbf{P}(t) = \mathbf{P}_\infty$ satisfies (11). Finally, consider the equation in (4) under the actual expression of $\mathbf{E}(t)$. Note that it differs from the nominal filter only in the perturbation given by the difference $\mathbf{E}(t) - \mathbf{E}_k$. Then, due to the asymptotic stability of the filter and using similar arguments as in [30, Lemma 9.3], both nominal and perturbed filters converge to the same value as $\lim_{t-t_k\to\infty} \mathbf{P}(t) = \mathbf{P}_\infty$ since the perturbation $\mathbf{E}(t) - \mathbf{E}_k$ vanishes as $t - t_k \to \infty$. ■

A. Discussion on Main Results

In Proposition 1 and Theorem 3, we have established the main properties of our DETM and EBSE.

In particular, Proposition 1 demonstrates that the probability of $\eta(t)$ taking large values is negligible, as indicated by the chi distribution bound $\bar{\eta}_k$. Studying the boundedness of $\eta(t)$ is crucial because it affects the triggering threshold for events, which is used in the matrix $\mathbf{E}(t)$ related to the negative information. However, the dynamics of $\eta(t)$ are affected by stochastic noise from the measurements, requiring a probabilistic bound for $\eta(t)$, in contrast to other works that do not consider stochastic noise.

Regarding Theorem 3, items 1) and 2) ensure a bounded mean-squared error for the estimate, preventing the uncertainty from diverging. This is a significant improvement compared to approaches relying solely on model-based predictions for interevent intervals in the stochastic context. Item 2) addresses the conservativeness introduced by negative information through an overestimated Gaussian noise $\mathbf{E}(t)$ in the EBSE. The estimate $\mathbf{P}(t)$ is an upper bound for the covariance of the error resulting from negative information. Item 3) indicates the asymptotic convergence of the uncertainty bound at an interevent interval.

Notice that, for the sake of clarity, the design and analysis of our filter have been carried out by assuming that negative information is available for the whole interval (t_k, t_{k+1}), i.e., as if the time regularization parameter $\underline{\tau} \to 0$ in (2). This is reasonable in practice, where $\underline{\tau}$ can be set small such as the actual sampling step of the sensor. For arbitrary $\underline{\tau} > 0$, there is an interval $(t_k, t_k + \underline{\tau})$ for which negative information is not available. However, we are mainly interested in preventing divergence of the uncertainty when a significant amount of time has elapsed since the last event. Hence, using $\underline{\tau} > 0$ does not compromise the main conclusions for our proposal.

Finally, note that we have performed the analysis of boundedness for our particular DETM, but it can be extended to other triggers by choosing the appropriate $\mathbf{E}(t)$, as explained in Section III-A. For Theorem 3 to hold, $\mathbf{E}(t)$ has to be bounded and known to the remote estimator for all t.

V. Implementation

Here, we provide some insights into the implementation process for our proposal. Note that using the DETM and EBSE combination requires the implementation of an algorithm at the sensor side, to check the dynamic event-triggering condition, and the estimation algorithm at the remote estimator.

In cyber–physical applications, the physical system generally operates in continuous time, and continuous measurements can be obtained through analog sensors. However, the system is managed digitally through computers. Thus, the continuous-time system is often approximated by algorithms running at a high frequency. Therefore, in the following algorithms, as well as in the simulation examples from Section VI, we use an arbitrarily small sampling step h to run the proposal in a digital platform. Henceforth, the differential equations in (2) and (4) are implemented using an explicit forward Euler discretization with time step h as evident when updating $\eta, \hat{\mathbf{x}}, \mathbf{P}$ in the following algorithms. Moreover, notice that this excludes Zeno behavior in practice: the sampling step forces a minimum interevent time, naturally acting as $\underline{\tau} > 0$ in the ETM (2).

Algorithm 1 summarizes the protocol at the sensor side, which consists of updating the dynamic variable in the ETM and checking the event-triggering condition. Note that, while this task requires some computing capabilities, the variable $\eta(t)$ is scalar and its update is less computationally demanding than other approaches requiring a copy of the Kalman filter at the sensor side. Algorithm 2 captures the operations at the estimator side, which runs the proposed hybrid EBSE. Moreover, note that the estimator side also keeps track of the value of $\eta(t)$ as in the sensor side, in order to use negative information. We have simplified the notations in the algorithms, omitting the time dependence and keeping a subindex k to denote the data from the latest event.

Algorithm 1: Algorithm at Sensor Side

Set discretization step h
Set parameters σ, ε, c_1, c_2, m_0, η_0 for the ETM (2)
Initialize ETM variables $\eta \leftarrow \eta_0$, $m_k \leftarrow m_0$
Set initial event $t_k \leftarrow 0$, $\mathbf{y}_k \leftarrow \mathbf{y}(0)$
for *each time step* t **do**
  Measure $\mathbf{y}$
  Update $\eta \leftarrow \eta + h(-c_1\eta + c_2 m_k)$
  if $\|\mathbf{y} - \mathbf{y}_k\| \geq \sigma\eta + \varepsilon$ *(event at time t)* **then**
    Send $\mathbf{y}$ to remote estimator
    Update ETM variables: $m_k \leftarrow \|\mathbf{y} - \mathbf{y}_k\|/(t - t_k)$, $\eta \leftarrow \eta_0$
    Update latest event data: $t_k \leftarrow t$, $\mathbf{y}_k \leftarrow \mathbf{y}$
  end
end

Algorithm 2: Algorithm at Estimator Side

Set system matrices $\mathbf{A}$, $\mathbf{B}$, $\mathbf{C}$, $\mathbf{W}$, $\mathbf{R}$
Set discretization step h
Set parameters σ, ε, c_1, c_2, m_0, η_0 as in sensor side
Initialize ETM variables $\eta \leftarrow \eta_0$, $m_k \leftarrow m_0$
Initialize estimates $\hat{\mathbf{x}} \leftarrow \mathbf{x}_0$, $\mathbf{P} \leftarrow \mathbf{P}_0$
Initial event $t_k \leftarrow 0$, $\mathbf{y}_k \leftarrow \mathbf{y}(0)$
for *each time step* t **do**
  Update $\eta \leftarrow \eta + h(-c_1\eta + c_2 m_k)$
  Update estimate with negative information from last event (4):
  $\mathbf{M} \leftarrow \mathbf{R} + (\sigma\eta + \varepsilon)^2\mathbf{I}_{n_\mathbf{y}}$
  $\mathbf{G} \leftarrow \mathbf{P}\mathbf{C}^\top\mathbf{M}^{-1}$
  $\hat{\mathbf{x}} \leftarrow \hat{\mathbf{x}} + h(\mathbf{A}\hat{\mathbf{x}} + \mathbf{G}(\mathbf{y}_k - \mathbf{C}\hat{\mathbf{x}})$
  $\mathbf{P} \leftarrow \mathbf{P} + h(\mathbf{A}\mathbf{P} + \mathbf{P}\mathbf{A}^\top + \mathbf{B}\mathbf{W}\mathbf{B}^\top - \mathbf{G}\mathbf{M}\mathbf{G}^\top)$
  if *new measurement* $\mathbf{y}$ *is received* **then**
    Update ETM variables: $m_k \leftarrow \|\mathbf{y} - \mathbf{y}_k\|/(t - t_k)$, $\eta \leftarrow \eta_0$
    Update latest event data: $t_k \leftarrow t$, $\mathbf{y}_k \leftarrow \mathbf{y}$
    Update estimate with new measurement (5):
    $\mathbf{L} \leftarrow \mathbf{P}\mathbf{C}^\top(\mathbf{C}\mathbf{P}\mathbf{C}^\top + \mathbf{R})^{-1}$
    $\hat{\mathbf{x}} \leftarrow \hat{\mathbf{x}} + \mathbf{L}(\mathbf{y}_k - \mathbf{C}\hat{\mathbf{x}})$
    $\mathbf{P} \leftarrow (\mathbf{I}_{n_\mathbf{x}} - \mathbf{L}\mathbf{C})\mathbf{P}$
  end
end

VI. Simulation Experiments

We have performed simulation experiments to validate our proposal and compare it to other methods. Consider a one-dimensional object tracking problem, in which the state vector contains the object's position $x(t)$ and velocity $v(t)$, i.e., $\mathbf{x}(t) = [x(t),\ v(t)]^\top$. The process is modeled as an integrator, with the matrices

$$\mathbf{A} = \begin{bmatrix} 0 & 1 \\ 0 & 0 \end{bmatrix},\ \mathbf{B} = \begin{bmatrix} 0 \\ 1 \end{bmatrix},\ \mathbf{C} = \begin{bmatrix} 1 & 0 \end{bmatrix}$$

and covariances $\mathbf{W} = 0.1$, $\mathbf{R} = 0.01$ for the process and measurement noise, respectively. Note that this linear system has two poles at the origin, making it unstable in the sense that a bounded input can cause an unbounded output. Thus, it has the effect of producing diverging uncertainties for the estimates when only a model prediction is used between events. Moreover, it can be verified that this system fulfills Assumption 1.

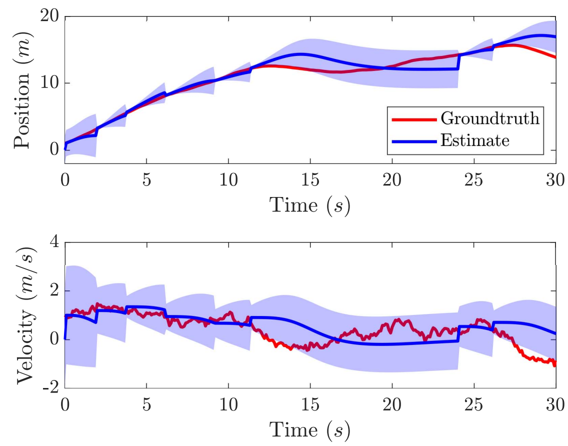

Fig. 2. Estimation results with DETM and EBSE (our proposal). It reduces communication compared to other triggers while keeping a bounded uncertainty between events.

The initial values for the trigger parameters have been arbitrarily set to $\eta_0 = m_0 = 1$, and the constants for the triggering condition $\sigma, \varepsilon, c_1, c_2 = 1$. The initial state $\mathbf{x}(0)$ follows a normal distribution with mean $\mathbf{x}_0 = [1, 1]^\top$ and covariance $\mathbf{P}_0 = \mathbf{I}_{n_\mathbf{x}}$. Since the initial conditions of the state are usually not known in practice, we initialize the estimates to $\hat{\mathbf{x}}(t_0^-) = [0, 0]^\top$, $\mathbf{P}(t_0^-) = \mathbf{I}_{n_\mathbf{x}}$. The system has been simulated using the Euler–Maruyama method, with a simulation step of $h = 0.1$ s, obtaining the ground-truth curves shown later in the results. Due to this discretization, we have selected a minimum interevent time of $\underline{\tau} = h$.

Through a comparison of different approaches, we aim to validate the following properties for our DETM and EBSE: 1) the proposed EBSE using negative information produces a bounded uncertainty regardless of the timing of transmissions, as opposed to using a standard Kalman prediction between events; 2) the proposed DETM adaptively reduces communication compared to static ETMs; and 3) our hybrid EBSE improves the results from previous sampled-data approaches using a more conservative inclusion of negative information.

Figs. 2–5 show the estimation results for several setups. The blue area in the figure represents the uncertainty around each coordinate estimate. Its width is set to be twice the uncertainty bound, in analogy to a standard confidence interval. In particular, Fig. 2 shows the result for our proposal, using the DETM in (2) and our EBSE in the remote estimator as in (4) and (5). It can be observed that the uncertainty of the estimates remains bounded even as interevent intervals become large, due to exploiting the negative information from the triggering condition. Moreover, note that for a large interevent interval (e.g., for $t \in (12, 24)$ in Fig. 2) the uncertainty bound converges to a constant value. This is due to the asymptotic solution of $\mathbf{P}(t)$ given by a Riccati equation, as shown in item 3) of Theorem 3.

The bounded uncertainty in Fig. 2 is an improvement compared to Fig. 3, which shows the estimates using the same

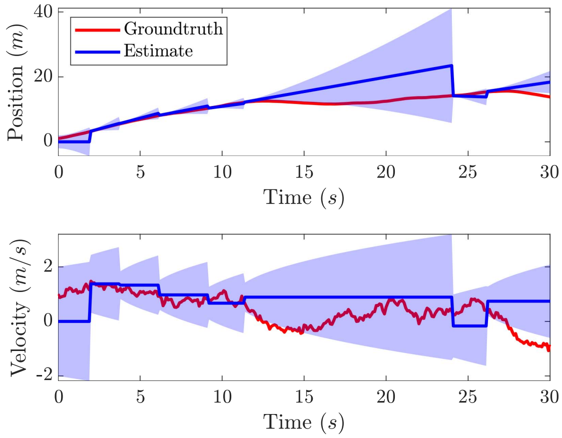

Fig. 3. Estimation results with DETM and KF. The uncertainty of the estimates diverges between events since negative information is not used.

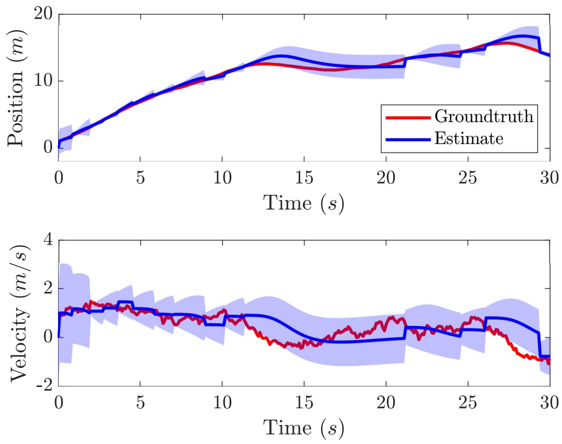

Fig. 4. Estimation results with SOD and EBSE. The uncertainty bound is smaller than with the DETM trigger, but at the cost of an increase in communication (double as DETM).

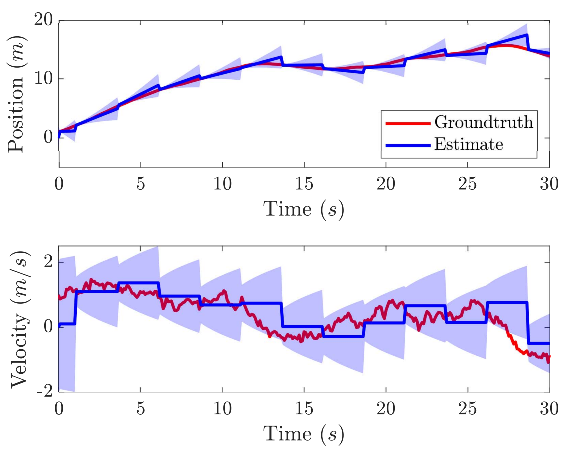

Fig. 5. Estimation results with VBT and KF. The trigger keeps the uncertainty bounded but results in periodic transmissions, regardless of the behavior of the measured signal.

DETM but with Kalman predictions between events (KF). This is, the model-based prediction from the last event is used, without taking advantage of the negative information. Due to the unstable system under consideration, the model-based prediction causes the uncertainty to increase without a uniform bound until a new measurement is received, leading to possibly large uncertainties, as can be seen for the interval $t \in (12, 24)$.

Fig. 4 shows the estimate produced with an SOD trigger [1], using our proposed EBSE with negative information. This configuration is subsumed in our approach as it corresponds to the case in which $\sigma = 0$ is set in (2). For this triggering rule, we have that $\mathbf{E}(t) = \varepsilon^2 \mathbf{I}_{n_y}$, and we set $\varepsilon = 1$ in this example. The main difference between the SOD and DETM is that the DETM provides an enlarged triggering threshold $\delta(t) \geq \varepsilon$, due to the addition of the dynamic variable. Accordingly, note that $\mathbf{E}(t)$ will take larger values for the DETM than for the SOD, due to its dependence on the magnitude of the event threshold $\delta(t)$, producing a larger uncertainty bound for the DETM. Nevertheless, the uncertainty is bounded for both setups, due to using our EBSE taking the negative information into account. Moreover, the smaller uncertainty bound for the SOD comes at the cost of a higher communication load. In this case, the DETM manages to reduce the number of events to half the amount for the SOD, thanks to the increased threshold.

Now, we compare with a variance-based trigger (VBT) [4], alongside the standard Kalman filter. Given that the variance is monitored in the triggering condition, this approach ensures that it remains uniformly bounded as well. In this case, a measurement is transmitted when its corresponding estimation variance exceeds a threshold

$$t_{k+1} = \inf\left\{ t - t_k > \underline{\tau} \;\; \middle| \;\; \mathrm{tr}(\mathbf{C}\mathbf{P}(t|t_k)\mathbf{C}^\top + \mathbf{R}) \geq \varepsilon \right\}$$

where $\mathbf{P}(t|t_k)$ denotes the estimation covariance of $\mathbf{x}(t)$, given measurements obtained up until $t_k < t$. Note that, for a linear time-invariant system, the VBT can be seen as a *predictive* approach, as $\mathbf{P}(t|t_k)$ is computed as a model-based prediction from the information available until the event t_k. Note that the prediction only depends on the constant matrices $\mathbf{A}$, $\mathbf{B}$, $\mathbf{W}$ and the time elapsed since t_k. As a consequence, the VBT results in periodic transmission of measurements, as shown in Fig. 5, where we present the estimates obtained with $\varepsilon = 1$. Hence, this approach does not take into consideration the current behavior of the signals, only the prediction for the covariance of the estimates. For this reason, the VBT may not provide an advantage in reducing communication in some cases where it would not be needed, such as when the measured signal is flat, given that its evolution is not monitored in the triggering condition. In Fig. 5, it can be seen that interevent intervals remain the same in steady state, regardless of the ground-truth signal having a steep or flat slope.

Additionally, recall that the VBT strategy requires the sensor node to run a local copy of the remote estimator, in order to estimate $\mathbf{P}(t|t_k)$ via a Kalman prediction. In contrast, using our EBSE instead of a regular Kalman filter ensures that uncertainty also remains bounded, while allowing the use of simpler triggering rules that monitor the current measured signal, achieving an adaptive behavior. Besides, the SOD and the proposed DETM do not require much computing power from the sensor side, as there is no need to run a copy of the Kalman filter, which may be especially costly for high-dimensional systems.

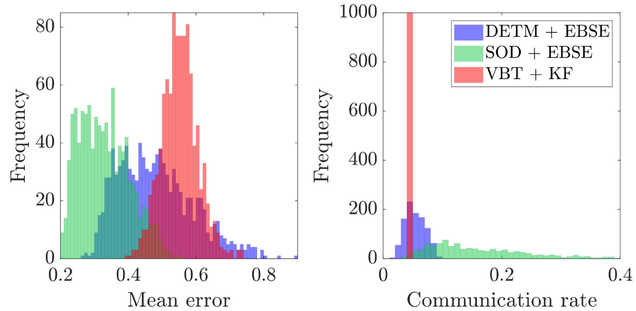

Fig. 6. Mean error and communication rate obtained for $N = 1000$ simulations of different trigger and estimator pairs. Our proposal (DETM + EBSE) achieves a better tradeoff between estimation error and reduction in communication compared to the SOD. It also adapts the communication rate as needed, in contrast to the VBT trigger which always results in the same fixed communication rate.

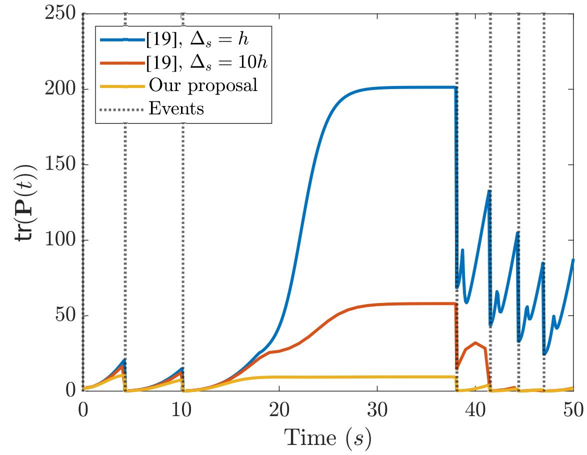

Fig. 7. Comparison of the estimated uncertainty bound for the EBSE in [19], with different periods Δ_s for the synchronous instants, and our proposal, with the same trigger for both. The estimates obtained with our proposal are independent from the sampling period Δ_s of the controller. Less conservative results are obtained for large interevent intervals and the instants after them, compared to [19].

To provide a more in-depth numerical comparison, we conducted $N = 1000$ simulations for each approach, with identical configurations and parameters, accounting for stochastic noise in the system. For each simulation, we have computed the mean error and communication rate as

$$\text{Mean error} = \frac{1}{T_f}\int_0^{T_f} \left\|\mathbf{x}(\tau) - \hat{\mathbf{x}}(\tau)\right\| d\tau$$

$$\text{Communication rate} = \frac{hE}{T_f}$$

where E is the number of events, h is the simulation step, and T_f is the total time of the experiment set to $T_f = 100$ s.

In this setup, we have obtained the histograms shown in Fig. 6, which illustrate the behavior of each approach. In the experiments, we have set the same $\varepsilon = 1$ for our DETM and the SOD. It can be observed that our DETM achieves a significant reduction in communication between the sensor and estimator compared to the SOD trigger, even though this increases the estimation error, as expected due to the tradeoff between communication and estimation quality. This tradeoff can be exploited by varying σ, reaching the same error performance as the SOD with $\sigma = 0$. Additionally, the communication rates for the SOD approach have higher variance than the DETM, while the error variance remains similar. In this experiment, the DETM achieves communication rates in the range [0.01, 0.1] while the communication rates for the SOD are spread out over the range [0.02, 0.4]. The SOD's fixed triggering threshold leads to a uniform sensitivity to changes in the measured signal, possibly resulting in excessive or insufficient events in different scenarios. Thus, the SOD requires a careful hand-tuning of the parameter ε so that it is appropriate for the magnitude of the measured signal, to achieve the desired tradeoff between communication and error. In contrast, our DETM adjusts the triggering threshold based on the measured signal's behavior, ensuring a relatively low communication rate for all cases, without requiring further adjustment. Note that this also validates the fact that reducing the number of events through a DETM is advantageous compared to simply setting a larger constant threshold ε in the SOD. While both options would reduce communication, the DETM does it adaptively, achieving better performance.

Fig. 6 shows that the VBT achieves comparable estimation errors to our DETM, but its communication rate remains fixed for all simulations. This is due to monitoring the *predicted* variance in the triggering condition, which has a known evolution over time that does not depend on the current behavior on the measured signals or state estimates. Moreover, for the linear time-invariant system under consideration, the predicted variance depends on the constant matrices $\mathbf{A}$, $\mathbf{B}$, $\mathbf{W}$, $\mathbf{C}$, $\mathbf{R}$, which results in periodic behavior and a constant communication rate for the experiments. In contrast, our DETM dynamically adapts communication based on the measured signal's evolution, reducing the number of triggered events as needed.

Finally, we also compare our results with the EBSE in [19], which is a similar negative information approach to ours, in terms of producing a mean estimate $\hat{\mathbf{x}}(t)$ and an uncertainty bound for the estimation error, and considering deterministic ETMs. To make a fair comparison of the estimators, we stick to using a simple event-triggering condition. In particular, we choose an SOD trigger, which was also tested in [19] with their own EBSE. We set the threshold to $\delta = 5$. Recall from Section III-B that the main differences of [19] compared to our work were the use of ellipsoidal representations for negative information at interevent intervals rather than a Gaussian approximation, and incorporating negative information at some synchronous instants (the sampling period of the controller that receives the state estimates) rather than continuously. Fig. 7 shows the trace of the uncertainty bound for both approaches. We have simulated the EBSE in [19] for two values of the sampling period of the controller, with h being the simulation step and Δ_s being the synchronous period. We denoted the uncertainty as $\mathbf{P}(t)$, but it includes both the stochastic and deterministic terms $\mathbf{P}(t)$ and $\mathbf{X}(t)$ in [19].

The results show that our EBSE provides less conservative results when interevent intervals are large [e.g., in the interval $t \in (10, 38)$]. After a long time without events, our EBSE may also yield smaller uncertainties at event instants, as it happens for $t \geq 38$s in this example. It is mentioned in [19] that the Gaussian approximation of negative information can lead to optimistic results. However, when comparing our EBSE with other methods (e.g., Figs. 4 and 5), underestimation of the error is not observed. Moreover, recall that we showed the conservativeness of our approximation in Theorem 3.

Additionally, the results obtained for the approach in [19] show that the sampling period of the downstream controller can impact the estimation results for the EBSE, with the value of $\mathbf{P}(t)$ converging to different values according to the period Δ_s, since negative information is only considered at the periodic instants. In contrast, our hybrid approach makes use of all available information by incorporating negative information in a continuous form, eliminating this issue.

VII. Conclusion

We have presented a novel DETM and EBSE pair for remote state estimation, which allows reduced communication between the sensor and the remote estimator while keeping the uncertainty of the estimates bounded for all time in the presence of stochastic noise. We have shown the absence of Zeno behavior and the boundedness of the dynamic variable in the DETM via a study of its probability distribution. In addition, we have demonstrated the boundedness and asymptotic convergence of the uncertainty of the state estimates even when a new event is not triggered. Simulation experiments show better performance at interevent intervals than in the case of not using negative information, as well as improvements in comparison to the EBSE in [19]. In addition, we show a reduction in communication compared to other methods in the literature, including the static analogous to our DETM. Extending the proposal to a distributed estimation setup is not straightforward, particularly in terms of incorporating the negative information, and is left as future work.

References

[1] M. Miśkowicz, "Event-based sampling strategies in networked control," in *Proc. 10th IEEE Workshop Fact. Commun. Syst.*, 2014, pp. 1–10.

[2] J. Wu, Q. S. Jia, K. H. Johansson, and L. Shi, "Event-based sensor data scheduling: Trade-off between communication rate and estimation quality," *IEEE Trans. Autom. Control*, vol. 58, no. 4, pp. 1041–1046, Apr. 2013.

[3] L. Li, M. Lemmon, and X. Wang, "Event-triggered state estimation in vector linear processes," in *Proc. Am. Control Conf.*, 2010, pp. 2138–2143.

[4] S. Trimpe, "Event-based state estimation: An emulation-based approach," *IET Control Theory Appl.*, vol. 11, no. 11, pp. 1684–1693, 2017.

[5] X. Yin and J. Liu, "Event-triggered state estimation of linear systems using moving horizon estimation," *IEEE Trans. Control Syst. Technol.*, vol. 29, no. 2, pp. 901–909, Mar. 2021.

[6] X. Yin and B. Huang, "Event-triggered distributed moving horizon state estimation of linear systems," *IEEE Trans. Syst., Man, Cybern., Syst.*, vol. 52, no. 10, pp. 6439–6451, Mar. 2021.

[7] G. Battistelli, L. Chisci, and D. Selvi, "A distributed Kalman filter with event-triggered communication and guaranteed stability," *Automatica*, vol. 93, pp. 75–82, Jul. 2018.

[8] Q. Voortman, D. Efimov, A. Y. Pogromsky, J. P. Richard, and H. Nijmeijer, "An event-triggered observation scheme for systems with perturbations and data rate constraints," *Automatica*, vol. 145, Nov. 2022, Art. no. 110512.

[9] S. Trimpe and R. D'Andrea, "Event-based state estimation with variance-based triggering," *IEEE Trans. Autom. Control*, vol. 59, no. 12, pp. 3266–3281, Dec. 2014.

[10] S. Trimpe and M. C. Campi, "On the choice of the event trigger in event-based estimation," in *Proc. 1st Int. Conf. Event-Based Control, Commun. Signal Process.*, 2015, pp. 1–8.

[11] X. Ge, Q. L. Han, X. M. Zhang, and D. Ding, "Dynamic event-triggered control and estimation: A survey," *Int. J. Autom. Comput.*, vol. 18, no. 6, pp. 857–886, 2021.

[12] L. Ma, Z. Wang, C. Cai, and F. E. Alsaadi, "Dynamic event-triggered state estimation for discrete-time singularly perturbed systems with distributed time-delays," *IEEE Trans. Syst., Man, Cybern., Syst.*, vol. 50, no. 9, pp. 3258–3268, Sep. 2020.

[13] Y. Niu, L. Sheng, M. Gao, and D. Zhou, "Dynamic event-triggered state estimation for continuous-time polynomial nonlinear systems with external disturbances," *IEEE Trans. Ind. Informat.*, vol. 17, no. 6, pp. 3962–3970, Jun. 2021.

[14] E. Petri, R. Postoyan, D. Astolfi, D. Nesic, and W. P. M. H. Heemels, "Event-triggered observer design for linear systems," in *Proc. 60th IEEE Conf. Decis. Control*, 2021, pp. 546–551.

[15] D. Zhao, Z. Wang, G. Wei, and Q.-L. Han, "A dynamic event-triggered approach to observer-based PID security control subject to deception attacks," *Automatica*, vol. 120, Oct. 2020, Art. no. 109128.

[16] D. Ding, Z. Wang, and Q. L. Han, "A set-membership approach to event-triggered filtering for general nonlinear systems over sensor networks," *IEEE Trans. Autom. Control*, vol. 65, no. 4, pp. 1792–1799, Apr. 2020.

[17] J. Li, X. Liu, X. Su, B. Liu, and J. Liu, "H_∞ filtering of repeated scalar nonlinear systems: Event-triggered communication case," *IEEE Trans. Syst., Man, Cybern., Syst.*, vol. 51, no. 6, pp. 3392–3400, Jun. 2021.

[18] K. Zhu, Z. Wang, H. Dong, and G. Wei, "Set-membership filtering for two-dimensional systems with dynamic event-triggered mechanism," *Automatica*, vol. 143, Sep. 2022, Art. no. 110416.

[19] J. Sijs, B. Noack, and U. D. Hanebeck, "Event-based state estimation with negative information," in *Proc. 16th Int. Conf. Int. Soc. Inf. Fus. (ISIF)*, 2013, pp. 2192–2199.

[20] D. Shi, T. Chen, and L. Shi, "On set-valued Kalman filtering and its application to event-based state estimation," *IEEE Trans. Autom. Control*, vol. 60, no. 5, pp. 1275–1290, May 2015.

[21] K. Lu, R. Zhou, and H. Li, "Event-triggered cooperative target tracking in wireless sensor networks," *Chin. J. Aeronaut.*, vol. 29, no. 5, pp. 1326–1334, 2016.

[22] D. Han, Y. Mo, J. Wu, S. Weerakkody, B. Sinopoli, and L. Shi, "Stochastic event-triggered sensor schedule for remote state estimation," *IEEE Trans. Autom. Control*, vol. 60, no. 10, pp. 2661–2675, Oct. 2015.

[23] L. Li, M. Niu, Y. Xia, and H. Yang, "Stochastic event-triggered distributed fusion estimation under jamming attacks," *IEEE Trans. Signal Inf. Process. Over Netw.*, vol. 7, pp. 309–321, Apr. 2021.

[24] H. Yu, J. Shang, and T. Chen, "On stochastic and deterministic event-based state estimation," *Automatica*, vol. 123, Jan. 2021, Art. no. 109314.

[25] T. Soderstrom, *Discrete-Time Stochastic Systems: Estimation and Control*, 2nd ed. Berlin, Germany: Springer, 2002.

[26] M. Miskowicz, *Event-Based Control and Signal Processing*. London. U.K.: Routledge, 2016.

[27] B. D. Anderson and J. B. Moore, *Optimal Filtering* (Prentice-Hall Information and System Sciences Series). North Chelmsford, Ma, USA: Courier Corp., 1979.

[28] R. E. Kalman and R. S. Bucy, "New results in linear filtering and prediction theory," *ASME J. Fluids Eng.*, vol. 83, no. 1, pp. 95–108, 1961.

[29] N. Thacker and T. Lacey, *Tutorial: The Kalman Filter*, Imag. Sci. Biomed. Eng. Div., Med. School, Univ. Manchester, Manchester, U.K., vol. 61, 1998.

[30] H. K. Khalil, *Nonlinear Systems*, 3rd ed. Hoboken, NJ, USA: Prentice Hall, 2002.

Irene Perez-Salesa (Graduate Student Member, IEEE) received the B.S. degree in industrial engineering technology and the M.S. degree in industrial engineering from the University of Zaragoza, Zaragoza, Spain, in 2019 and 2021, respectively, where she is currently pursuing the Ph.D. degree in computer science and systems engineering.

Her research interests include distributed estimation and control, and event-triggered communication protocols.

Rodrigo Aldana-López (Graduate Student Member, IEEE) received the B.S. degree in electronics engineering from the Instituto Tecnológico y de Estudios Superiores de Occidente, Tlaquepaque, Mexico, in 2016, and the Ph.D. degree in computer science and systems engineering from the University of Zaragoza, Zaragoza, Spain, in 2024.

His research interests include real-time robotics, machine learning, and communication protocols and control for distributed systems.

Carlos Sagüés (Senior Member, IEEE) received the M.S. degree in computer science and systems engineering and the Ph.D. degree in industrial engineering from the University of Zaragoza, Zaragoza, Spain, in 1989 and 1992, respectively.

In 1994, he joined as an Associate Professor with the Departamento de Informática e Ingeniería de Sistemas, University of Zaragoza, where he became a Full Professor in 2009, and was also the Head Teacher. He was engaged in research on force and infrared sensors for robots. His current research interests include control systems and industry applications, computer vision, visual control, and multivehicle cooperative control.